Combustion and Emission Performance of an HCCI Engine Fuelled by n-Heptane/Toluene Blends at a Low-Load Operating Condition

Hongsheng Guo* and W. Stuart Neill

Energy, Mining and Environment Research Center, National Research Council Canada, 1200 Montreal Road, Ottawa, Ontario K1A 0R6

Abstract: Homogeneous charge compression ignition (HCCI) engine technology offers high fuel efficiency and extra low nitrogen oxide (NO_x) and particulate matter (PM) emissions, which makes it a potential alternative combustion mode to conventional diesel engines. A diesel fuel is usually composed of many classes of hydrocarbons among which aromatic compounds have attracted special attention due to their specific combustion characteristics. Understanding the combustion and emission characteristics of different classes of hydrocarbons is crucial for identifying appropriate diesel fuels suitable for HCCI combustion. Toluene is a typical aromatic compound in a diesel fuel. A study of toluene content may provide implications of the effect of aromatic in a diesel fuel on HCCI combustion.

In this paper, the combustion and emission performance of an HCCI engine fuelled by n-heptane/toluene blends at a low load operating condition was investigated by experiment and numerical simulation. A modified Cooperative Fuel Research (CFR) engine and a in-house-developed multi-zone model were employed. The engine was operated at the condition of engine speed of 900 rpm, relative air/fuel ratio of 3.5 and without external exhaust gas recirculation. The investigated fuel blends covered a range from pure n-heptane to 70% toluene by volume. Both experimental and numerical results showed that an increase in toluene fraction in the fuel blend retarded combustion phasing. As a result, the optimal compression ratio, at which thermal efficiency reached its maximum for a fuel blend, increased with increasing toluene fraction. The maximum thermal efficiency increased as the toluene fraction increased from 0 to 50%, but then decreased with further increasing toluene fraction to higher values. The peak pressure rise rate also increased with increasing toluene fraction at a constant combustion phasing. An increase in toluene fraction resulted in an increase in unburned hydrocarbon emissions but had little effect on NO_x emissions.

Keywords: Internal combustion engine, HCCI, Diesel combustion, Aromatics.

1. INTRODUCTION

Homogeneous charge compression ignition (HCCI) engine technology may offer the opportunity to have high fuel efficiency while virtually eliminating nitrogen oxide (NO_x) and particulate matter (PM) emissions [1-3]. The disadvantages of HCCI combustion are high carbon monoxide (CO) and unburned hydrocarbon emissions, along with high peak pressures and high rates of heat release [4]. It is of great importance to control the combustion of an HCCI engine so that the advantages can be maintained while the disadvantages are overcome as much as possible. Since it has been well known that HCCI combustion is mainly controlled by chemical kinetics [3], appropriate fuels that allow an HCCI engine to operate at optimal conditions are key to the development of the technology.

Diesel engines are widely used in transportation and off-road vehicles. The advantages of HCCI combustion make it a potential alternative combustion mode to conventional diesel engines [5]. A commercial diesel fuel is usually composed of many classes of hydrocarbons, such as alkanes, iso-alkanes, alkenes, and aromatics. Understanding the combustion and emission characteristics of different classes of hydrocarbons is crucial for identifying appropriate diesel fuels suitable for diesel HCCI combustion as well as for the development and design of HCCI engines. Among the classes of hydrocarbons in a diesel fuel, aromatic compounds have attracted special attention due to their specific combustion characteristics. The content of aromatic compounds in a diesel fuel has been identified as a specific fuel property that my significantly affect the combustion and emission characteristics of a diesel fuel [6].

Toluene is a typical aromatic compound. A study of toluene content may provide implications of the effect of aromatic content in a diesel fuel. Some studies [7, 8] have identified toluene as the representative of aromatics in forming a surrogate kinetic mechanism for diesel or gasoline combustion. Therefore, a study on the effect of toluene content in a diesel fuel can also provide data base for the validation of surrogate kinetics mechanisms of diesel combustion.

Sakai *et al*. [9] reported a study on the ignition delay times of primary reference fuel and toluene mixtures behind reflected shock waves and found that the ignition delay times of n-heptane increased with the

*Address correspondence to this author at the National Research Council Canada, 1200 Montreal road, Ottawa, Ontario K1A 0R6, Canada;
Tel: 1-613-991-0869; Fax: 1-613-957-7869;
E-mail: Hongsheng.guo@nrc-cnrc.gc.ca

E-ISSN: 2409-5826/18

addition of toluene. Xiao *et al*. [10] studied the effects of fuel aromatic and oxygenate compounds on exhaust emissions in a conventional diesel engine at a constant engine operation condition. They found that fuel blends containing toluene caused a significant increase in both NO_x and PM emissions, in comparison with the emissions when the engine was running on 100% n-heptane. Szybist and Bunting [11] experimentally investigated the effects of fuel composition on thermal efficiency in an HCCI engine at various compression ratios and concluded that the higher toluene content in fuels did not significantly change thermal efficiency. However, emission characteristics were not investigated in [11].

In this paper, a comprehensive study on the combustion and emission characteristics of an HCCI engine fuelled by various n-heptane/toluene blends is conducted by experiment and numerical simulation at a wide range of compression ratio. The purpose is to systemically study the effect of the variation in toluene content in a diesel on the performance of an HCCI engine. Numerical simulation is conducted together with experiments to confirm experimental data. n-Heptane is selected as the base fuel because it is a primary diesel reference fuel. The paper starts with the introduction of experimental setup and procedure, followed by a brief description of the numerical model. Then the results are presented and discussed. Finally, conclusions are drawn.

2. EXPERIMENTAL SETUP AND PROCEDURE

A Cooperative Fuel Research (CFR) engine was used for the experiments. It is a single-cylinder, four-stroke, variable compression ratio engine. The engine setup was modified from the original CFR engine by the addition of an air-assisted port fuel injection system and the hardware to control important engine parameters, such as intake temperature, air/fuel ratio, intake and exhaust pressures, and exhaust gas recirculation (EGR). The schematic diagram of the engine facility is shown in Figure **1**. The basic engine specifications are listed in Table **1**.

A port fuel injector (vaporizer) was used to atomize the fuels just upstream of the intake port. Compressed air, taken from the intake air after the mass flow meter, was used as blast air to improve the atomization process. For this study, the fuel and air-blast pressures were maintained at 500 kPa and 200 kPa, respectively. The timing and duration of the air blast relative to the fuel injection was optimized to minimize emissions. This fuel injector produced droplets with approximately 15 μm Sauter mean diameter under the conditions used in this study. A heated section was added directly downstream of the fuel injector to increase the fuel spray temperature and partially vaporize the fuels before they enter the cylinder. This helped to improve the fuel-air mixing process during the compression stroke. The exit temperature of the fuel vaporizer (T_{vap}) was maintained at a constant value of 220 ^{o}C in the

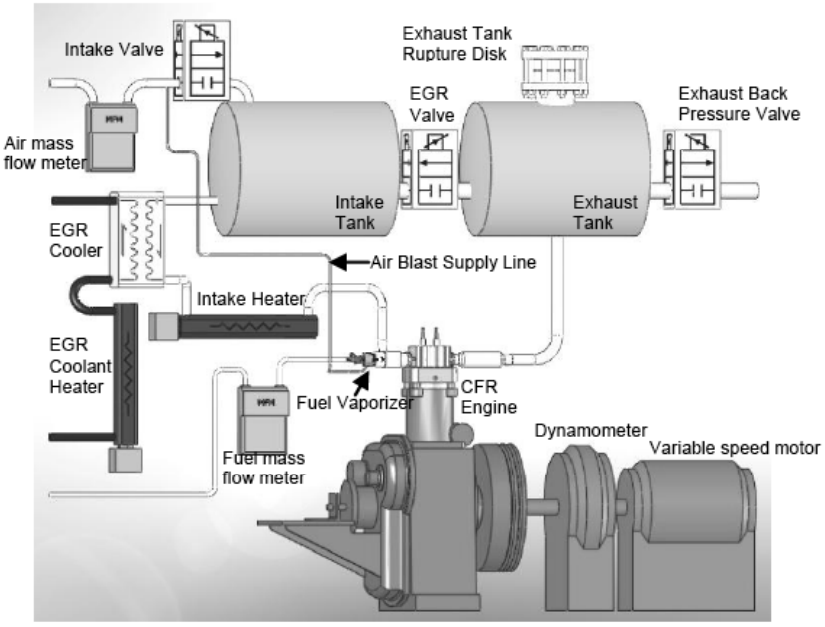

Figure 1: Schematic diagram of the engine research facility.

experiments. Further details about the fuel injector can be found elsewhere [6].

Table 1: Engine Specifications

Cylinder Bore	8.255 cm
Stroke	11.43 cm
Displacement Volume	611.7 cm^3
Connection Road Length	25.4 cm
Compression Ratio	6 ~ 16
Combustion chamber	Pancake shape, flat top piston
Intake valve open Intake valve close Exhaust valve open Exhaust valve close	10 ^oCA ATDC* 34 ^oCA ABDC 40 ^oCA BBDC 5 ^oCA ATDC
Fuel System	Air-assisted port fuel injection

*ATDC: after top dead center.

The intake air was provided from a pressurized dry air source and was measured by a mass flow meter before entering the intake surge tank, where the air was mixed with recycled exhaust gases. The engine exhaust was routed to an exhaust surge tank equipped with a safety rupture disk. A back pressure valve was used to maintain the exhaust pressure slightly above the intake pressure to provide the pressure difference needed to recycle exhaust gas to the intake stream. The EGR rate was defined as the ratio of the CO_2 volume fraction in the intake mixture to that in the exhaust.

For each experiment, the n-heptane/toluene fuel mixture was mixed inside a tank according to the blend ratio. Air/fuel mass ratio (AFR) was calculated based on the measured air mass flow rate and the measured n-heptane/toluene mixture mass flow rate. The stoichiometric air/fuel ratio was calculated by taking into account the toluene/n-heptane blend ratio.

An engine data acquisition and control system (Sakor Technologies Inc., DynoLab™) was used to acquire temperatures, pressures, and flow rates. Exhaust gas composition was measured by an emission analyzer (California Analytical Instruments, 600 series). Indicated specific emissions were calculated by using the direct exhaust emission measurement and assuming equal mass flow rates for intake and exhaust.

A water-cooled pressure transducer (Kistler Corp., model 6041A) flush-mounted in the cylinder head was used to measure cylinder pressure. A real-time combustion analysis system (AVL LIST GmbH, IndiModule) was used to collect cylinder pressure data with 0.2 ^oCA resolution at each test condition. For each operation condition, the data for three hundred consecutive engine cycles were collected. All combustion-related parameters were first calculated for each individual cycle and then averaged for the 300 cycles, including indicated mean effective pressure (IMEP), coefficient of variation of IMEP (COV_{IMEP}), and the peak pressure rise rate ($dP/d\theta_{max}$), etc.

More details about the engine setup can be found elsewhere [12].

Different n-heptane/toluene blends were investigated. The toluene fraction in each fuel blend is defined as:

$$\alpha_{tol} = V_{tol} \Big/ \left(V_{tol} + V_{n-hep\tan e} \right) \quad (1)$$

with V_{tol} and $V_{n\text{-}heptane}$ being the liquid volumes of toluene and n-heptane, respectively. In total, five fuel blends, α_{tol} = 0%, 10%, 30%, 50% and 70%, were studied.

At each toluene fraction, a compression ratio sweep was conducted, while all other engine parameters were held constant. The low and high limits for compression ratio sweep were determined by a COV_{IMEP} of 5% and a peak pressure rise rate of 10 bar/^oCA, respectively. For all the studied cases, the engine parameters of intake pressure, exhaust pressure and intake mixture temperature were kept constant at 150 kPa, 170 kPa and 75 ^oC, respectively.

A low-load operating condition was used for the experiments, whereby engine speed = 900 rpm, EGR = 0% and λ = 3.5, with EGR and λ being the exhaust gas recirculation rate and the relative mass air/fuel ratio, respectively. Table **2** lists the detailed engine operation parameters in the experiment.

Table 2 Engine Specification and Operation Parameters

Engine speed	900 rpm
Intake pressure	150 kPa
Exhaust pressure	170 kPa
Intake mixture temperature (T_{mix})	75 ^oC
Vaporizer exit temperature (T_{vap})	220 ^oC
(EGR, λ)	(0%, 3.5)
Toluene fraction (α_{tol})	0 ~ 70%
Compression ratio	varied

3. NUMERICAL MODEL

A multi-zone model was employed to simulate the engine performance. The model assumes the working fluid to be an ideal gas and simulates a full four-stroke cycle of engine operation, starting from top dead center (TDC) during the exhaust stroke and finishing at the same point after the intake, compression, combustion and exhaust strokes, *i.e*. from -360 degrees to 360 degrees (ATDC - after top dead center).

Eight zones were used in the model, including one crevice zone (zone 1), one boundary zone (zone 2) and six core zones (zones 3 – 8). The model assumes that chemical reactions never happen in the crevice zone, and the temperature of the crevice zone is always lower than or equal to the cylinder wall temperature due to the large ratio of surface area to volume. The volume of the crevice zone was assumed to be constant as 2% of the clearance volume of the investigated engine. The mass distribution in the boundary zone and core zones was assumed to be a normal distribution, as shown in Figure **2**.

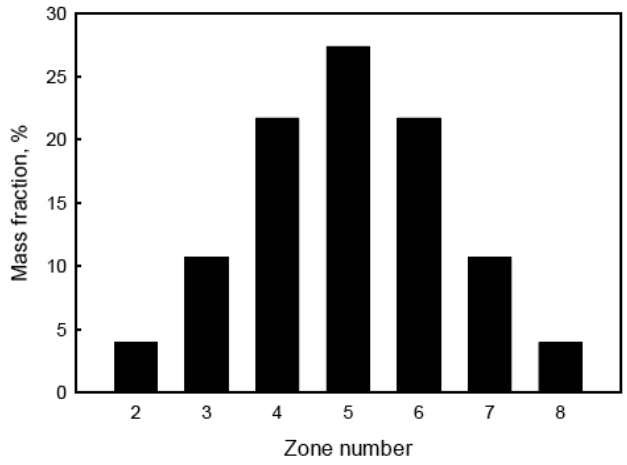

Figure 2: Mass distribution inside cylinder. Zone 2 is boundary zone, and others are core zones.

In the model, heat transfer between working fluid and cylinder wall happens through the boundary zone due to convection. Each core zone exchanges heat with its neighboring zones due to conduction and with cylinder wall due to radiation. Since the model assumes a constant crevice zone volume, there is mass exchange between crevice zone and other zones if pressure and temperature changes. To simplify the calculation, this mass exchange has been neglected during each time step. However, a mass adjustment is conducted after each time step. Then the adjusted masses are used during the next time step. The mass adjustment is conducted based on the total mass inside cylinder and the mass in the crevice zone. Before and after each time step, the mass of crevice zone can be calculated by the ideal gas state equation according to the crevice zone temperature, composition and cylinder pressure. Then the adjusted crevice zone mass Δm_{cre} can be obtained. During the pressure increase process, fluid flows from boundary zone and core zones to crevice zone, *i.e*. Δm_{cre} is positive. Oppositely, Δm_{cre} is negative during the pressure decrease (expansion) process. Further details of the model and the governing equations can be found elsewhere [13].

A kinetics mechanism developed by Andrae *et al*. [8] was used as the base chemistry. The NO_x formation chemistry in GRI Mech 3.0 [14] was added to the base chemistry to calculate NO_x emissions.

4. RESULTS AND DISCUSSION

Figure **3** shows the effect of toluene fraction in an n-heptane/toluene blend on pressure profile at a constant compression ratio (CR) of 12.0. The pressure profile for α_{tol} = 70% is absent in Figure **1** because stable combustion could not be obtained in both experiment and simulation for this blend at the compression ratio of 12.0. The results at other compression ratios were qualitatively similar. It reveals that the calculation reasonably reproduced the pressure profiles except for the case of α_{tol} = 50%. With an increase in toluene fraction in the fuel blend, both measurement and simulation showed that the peak pressure slightly decreased and the crank angle position at which pressure started to quickly increase retarded. The peak pressure was significantly underpredicted for the case of α_{tol} = 50% which was a near misfire condition. Although not shown, similar result was observed at other compression ratios, *i.e*. the peak pressure was

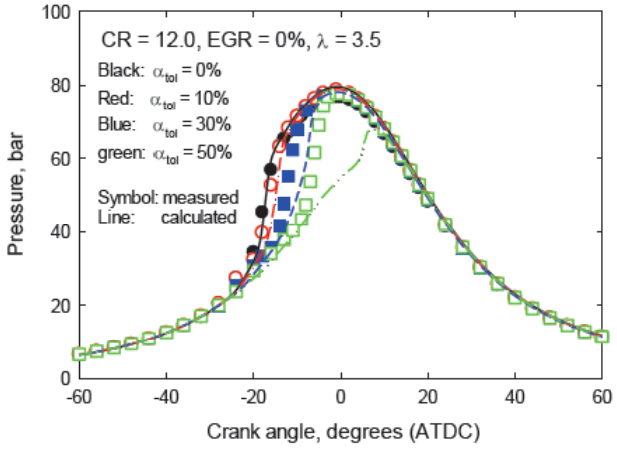

Figure 3: Pressure profiles at different n-heptane/toluene blends.

underpredicted when toluene fraction reached a high value that resulted in a near misfire condition. This suggests that the multi-zone model and/or kinetics mechanism used need further improvement for near misfire conditions, although they have been able to reasonably predict pressure profiles at most cases.

Combustion phasing is an important parameter that directly affects fuel conversion efficiency of an HCCI engine. Figure 4 shows the variation of the combustion phasing, defined as CA50 (the crank angle position at which 50% of cumulative heat release is reached), as a function of toluene fraction at compression ratios of 12.0 and 9.5. The results at other compression ratios were qualitatively similar. Both experiment and calculation showed that an increase in toluene fraction caused retardation of the combustion phasing at a constant compression ratio. This is qualitatively consistent with the observation of Sakai *et al*. [9] who found that the ignition delay of n-heptane in a shock tube increased with the addition of toluene. This was because n-heptane is a fuel with two stage-combustion, a low temperature heat release (LTHR) stage and a primary high temperature heat release (HTHR) stage, while toluene is a fuel whose combustion has little LTHR. The LTHR plays an important role in controlling the ignition process. When toluene fraction in the fuel blend increases, the heat release at LTHR stage reduces and the combustion phasing is retarded. Therefore, toluene is not as reactive as n-heptane in terms of ignition.

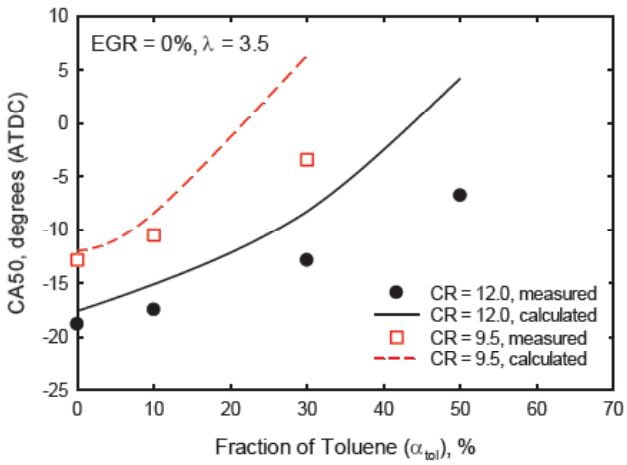

Figure 4: Variation of CA50 as a function of toluene fraction.

The variation of thermal efficiency, defined as the ratio of indicated work to total energy input to cylinder per engine cycle, is displayed as a function of toluene fraction at compression ratios of 12.0 and 9.5 in Figure **5**. Although quantitative differences exist, the calculation qualitatively captured the experimentally measured variation trend. With an increase in toluene fraction, thermal efficiency was improved at both compression ratios. Further, the rate of increase of thermal efficiency with increasing toluene fraction was higher at CR = 12.0 than at CR = 9.5. This was because an increase in toluene fraction helped optimize the combustion phasing. The higher cycle efficiency of an internal combustion engine is usually obtained when heat release happens near top dead center [15]. At compression ratios of 12.0 and 9.5, the combustion phasing was overly advanced relative to top dead center when the fuel was pure n-heptane, as shown in Figure **4**. With an increase in toluene fraction, the combustion phasing was gradually retarded. Therefore, more heat was released near top dead center and thus thermal efficiency was improved when the toluene fraction increased. The combustion phasing at CR = 9.5 was closer to top dead center than at CR = 12.0 for n-heptane and thus the extent in the improvement of combustion phasing optimization was less at CR = 9.5 than at CR = 12.0 when toluene fraction was increased. It should be pointed out that the increase of thermal efficiency with increasing toluene fraction at a constant compression ratio may not happen for all compression ratios, as will be discussed below. The quantitative difference in thermal efficiency between the measured and calculated results might be because the model could not capture the quantitative result of CO and HC emissions.

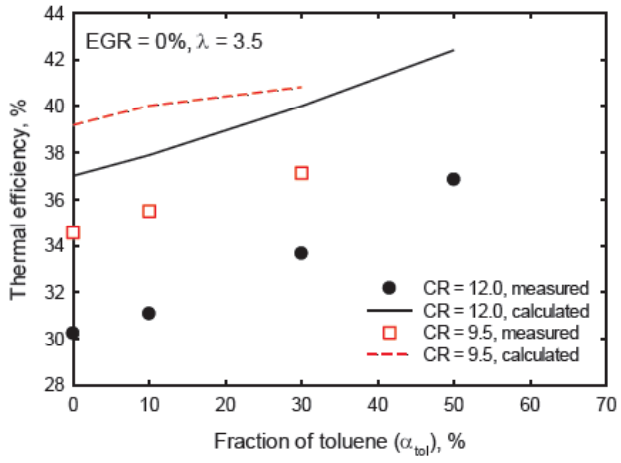

Figure 5: Variation of thermal efficiency as a function of toluene fraction at constant CRs.

Figure **6** displays the variation of thermal efficiency as a function of compression ratio for different fuel blends. It is noted again that the calculation successfully captured the qualitative variation trend. It first shows that the available data range along

horizontal axis (CR) narrowed with increasing toluene fraction. This suggests that the operational compression ratio window narrowed with increasing toluene fraction in the fuel blend, since the compression ratio sweep in our study for each fuel blend was conducted by limiting the low and high compression ratios according to COV_{IMEP} of 5% and the peak pressure rise rate of 10 bar/^{o}CA, respectively.

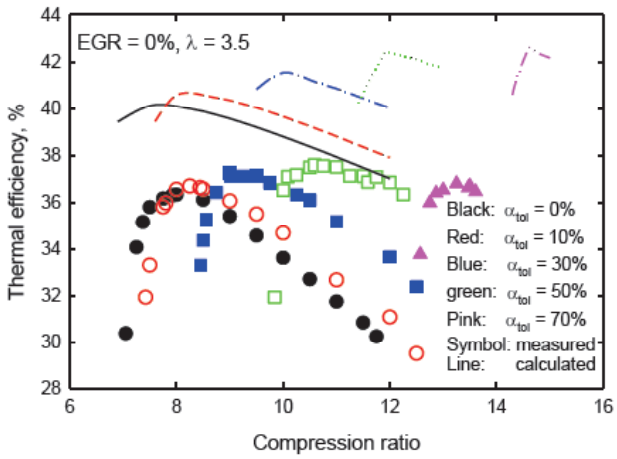

Figure 6: Variation of thermal efficiency for various fuel blends.

Figure **6** also shows that for each fuel blend, there was an optimal compression ratio at which the maximum thermal efficiency was reached. As the compression ratio was gradually decreased from a high value, thermal efficiency first increased until the maximum value was reached at the optimal compression ratio. This was because the combustion phasing was gradually retarded with decreasing compression ratio, as shown in Figure **4**, and thus more heat is released near top dead center. It was the more optimized combustion phasing rather than the lower compression ratio that leaded to an improved thermal efficiency for a given fuel blend when compression ratio decreased. However, further decreasing compression ratio decreased thermal efficiency due to overly retarded combustion phasing and engine misfire.

Thirdly, Figure **6** shows that the optimal compression ratio increased and the operational compression ratio window moved toward higher compression ratios with increasing toluene fraction. This was due to the fact that toluene is not as reactive as n-heptane in terms of ignition. Therefore, the optimal combustion phasing (usually around top dead center) occurred at a higher compression ratio with increasing toluene fraction. The movement of operational window toward higher compression ratios resulted in the fact that thermal efficiency did not always increase with increasing toluene fraction at a constant compression ratio, since a compression ratio that was within the operational window of one blend may be outside the operational window of other blends. Therefore, different operating compression ratio should be used when toluene fraction in a fuel blend changes.

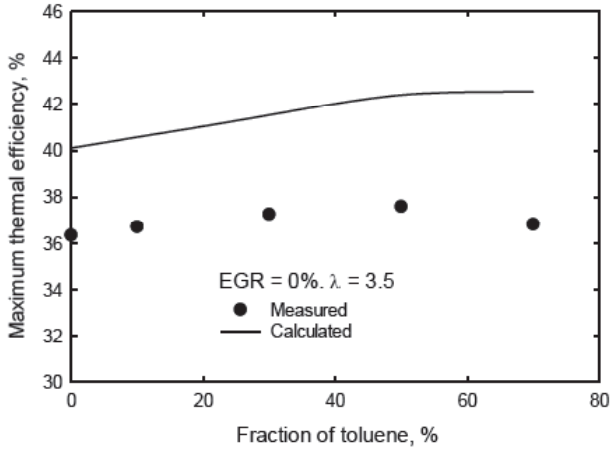

Figure 7: Variation of the maximum thermal efficiency as a function of toluene fraction.

Finally, as a result of the increase in optimal compression ratio, the maximum thermal efficiency increased with increasing toluene fraction from 0 to about 50%. This is clearly shown in Figure **7**. This increase in the maximum thermal efficiency with increasing toluene fraction is different from the result of Szybist and Bunting [11], who reported that the higher toluene fraction did not lead to a corresponding increase in thermal efficiency at a constant air/fuel ratio. The difference between our results and those of [11] might be due to the higher compression ratio used for the fuels with higher toluene fractions in our study. However, Figure **7** shows that a further increase in toluene fraction to above 50% caused the maximum thermal efficiency to decrease. The simulation also qualitatively captured this trend. This was because the combustion phasing became overly retarded when toluene fraction was high although a high compression ratio was used. It was observed in the experiment that COVIMEP became higher than 5% for fuel blends with toluene fraction higher than 70%. Therefore, there was an optimal toluene fraction in an n-heptane/toluene blend at which the best energy efficiency can be obtained.

Figure **8a** displays the variation of the peak pressure rise rate as a function of CA50 for various fuel

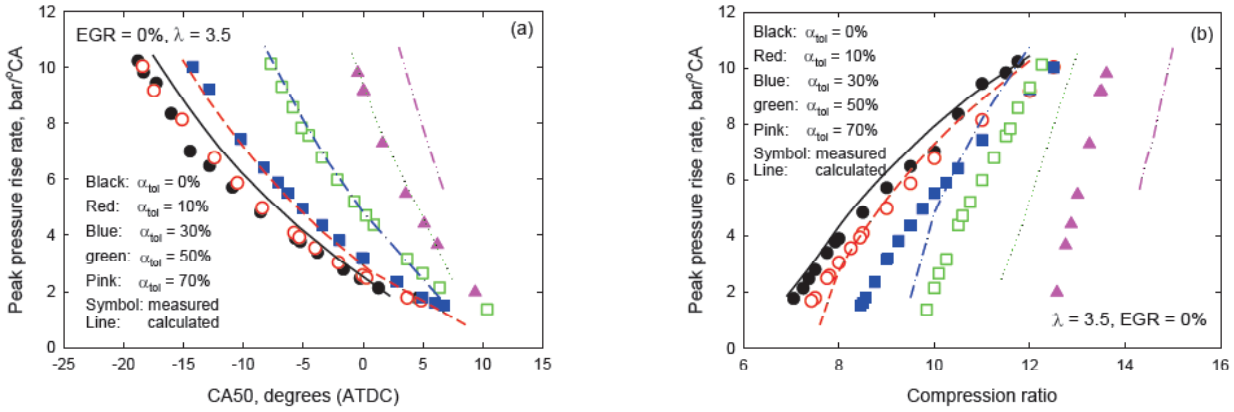

Figure 8: Variation of the peak pressure rise rate.

blends. Both measurement and calculation showed that as long as the combustion phasing was not overly retarded, the peak pressure rise rate increased with increasing toluene fraction at a constant combustion phasing, implying an intensified knock tendency with increasing toluene fraction in the fuel blend. Further, with increasing toluene fraction, the peak pressure rise rate became more sensitive to the variation of combustion phasing. However, the peak pressure rise rate decreased with increasing toluene fraction at a constant compression ratio, except for very high compression ratios, as shown in Figure **8b**. Therefore, the increase in the peak pressure rise rate with increasing toluene fraction at a constant combustion phasing was primarily due to the increased compression ratio, as discussed before.

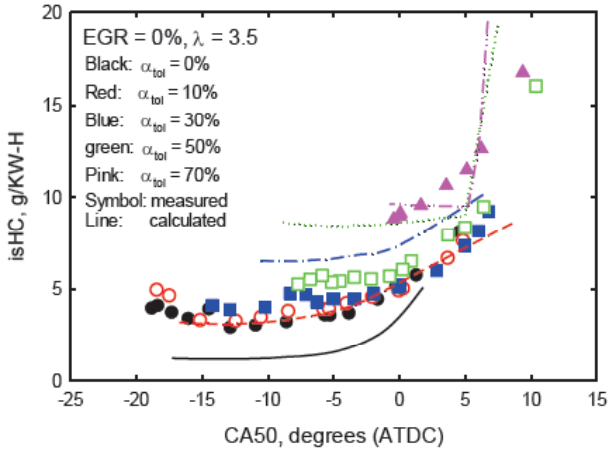

Figure 9: Variation of indicated specific unburned hydrocarbon (isHC) emissions.

The variation of indicated specific unburned hydrocarbon emissions as a function of CA50 is shown in Figure **9** for different fuel blends. It is observed that unburned hydrocarbon emissions increased at a constant combustion phasing with increasing toluene fraction although compression ratio was increased. This might be because toluene is not as reactive as n-heptane during ignition stage and more unburned hydrocarbons present at the primary high temperature heat release stage, which resulted in the increased unburned hydrocarbon emissions.

The variation of indicated specific NO_x emissions as a function of CA50 for various fuel blends is shown in Figure **10a**. It is noted that when the combustion phasing was advanced relative to top dead center, both measurement and calculation showed an increase in NO_x emissions with increasing toluene fraction at a constant combustion phasing. However, Figure **10b** shows that NO_x emissions decreased with increasing toluene fraction at higher constant compression ratios that resulted in the relatively advanced combustion phasing in Figure **10a**. This suggests that the increase in NO_x emissions with increasing toluene fraction at a constant advanced combustion phasing in Figure **10a** was primarily due to the increased compression ratio that led to the increase in cylinder temperature, as shown in Figure **11a** by the calculated temperature variations. The decrease in NO_x emissions with increasing toluene fraction at a constant high compression ratio was due to the decrease in cylinder temperature, as shown in Figure **11b**.

When the combustion phasing was retarded relative to top dead center or the compression ratio was lower, the calculation failed to reproduce the qualitative variation trend of NO_x emissions as toluene fraction increased. For retarded CA50 or lower compression ratios, the measurement suggested a decrease in NO_x emissions with increasing toluene fraction, while the calculation showed the opposite. It is not clear what

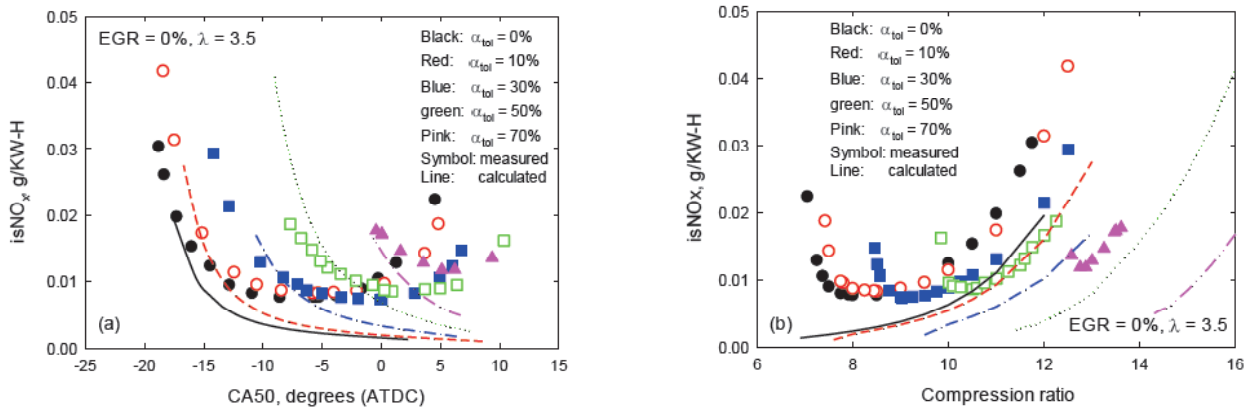

Figure 10: Variation of indicated specific NO_x emissions.

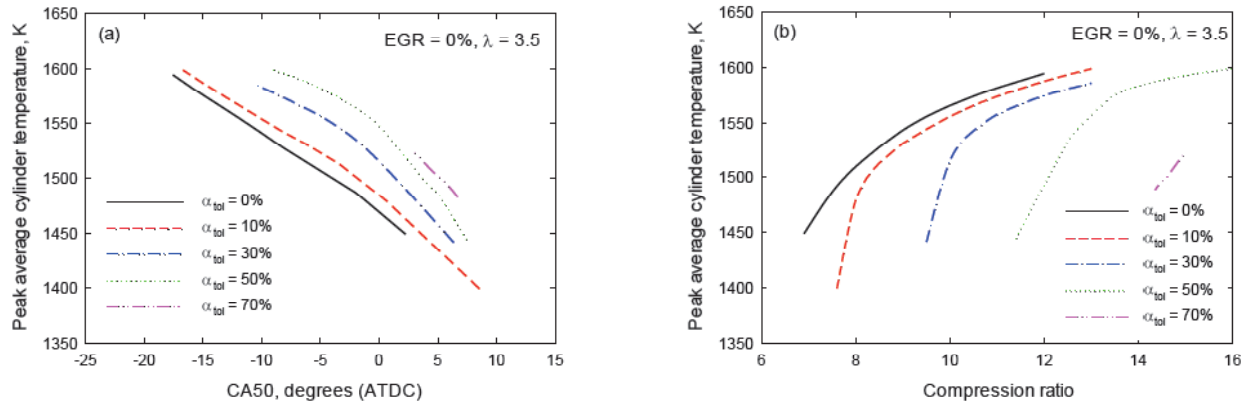

Figure 11: Calculated peak zone-averaged cylinder temperatures.

caused this qualitative difference between measured and calculated NO_x emission data for retarded CA50 or lower compression ratios. However, although the calculation showed a slight increase in NO_x emissions, the effect was very small at retarded CA50 or lower compression ratios. Further, if we consider that the optimal operational condition (when thermal efficiency was the highest) for each blend was usually when CA50 was around top dead center, Figure **11a** actually suggests that the variation of toluene fraction in the fuel blend has little effect on NO_x emissions at near optimal operational conditions. Therefore, we may conclude that increasing toluene fraction has negligible effect on NO_x emissions at near optimal operational conditions or retarded combustion phasing. This is different from the observation by Xiao *et al*. [10] who found that an increase in toluene fraction led to a significant increase in NO_x emissions in a conventional diesel engine.

The difference in NO_x emissions between this paper and [10] might be caused by the variation in NO_x formation mechanism in conventional and HCCI diesel engines. In a conventional diesel engine, combustion is diffusion or partially premixed process in which NO_x formation is usually dominated by prompt and/or thermal mechanism [16]. An increase in toluene fraction increases unburned hydrocarbon radicals during the primary high temperature heat release stage, as implied by Figure **9**, which may result in an increase in prompt NO_x formation. However, in an HCCI engine, combustion temperature is much lower and NO_x formation is dominated by the N_2O intermediate mechanism [17, 18], which is almost not affected by the presence of hydrocarbon radicals. As a result, the increase in toluene fraction has little effect on NO_x emissions in an HCCI engine.

CONCLUSIONS

The combustion and emission characteristics of an HCCI engine fuelled by n-heptane/toluene blends have been systemically investigated by experiment and numerical simulation. The engine was operated at the condition of engine speed = 900 rpm, λ = 3.5 and

EGR = 0%. A compression ratio sweep was conducted for each fuel blend and a self-developed multi-zone model was employed for the calculation of various engine operation cases. The numerical simulation qualitatively captured the experimentally observed variation trends of various combustion and emission data. From the results of experiment and simulation, the following conclusions are drawn.

1. When the kinetics mechanism developed by Andrae *et al*. [8] was coupled to a multi-zone model, the combustion and emission characteristics in HCCI engines fuelled by n-heptane/toluene fuel blends could be reasonably captured except for near misfire operating conditions when the mechanism and/or the multi-zone model may need further improvement;

2. An increase in toluene fraction in an n-heptane/toluene fuel blend retarded the combustion phasing in an HCCI engine;

3. The operational compression ratio window narrowed and moved toward higher compression ratios as toluene fraction increased in an n-heptane/toluene blend;

4. For each fuel blend, there was an optimal compression ratio at which thermal efficiency reached its maximum within the operational window. The optimal compression ratio also increased with increasing toluene fraction in the fuel blend;

5. The maximum thermal efficiency increased with increasing toluene fraction from zero to 50%, but decreased with further increasing toluene fraction at the operating conditions studied;

6. Although the peak pressure rise rate decreased at a constant compression ratio, it increased at a constant combustion phasing with increasing toluene fraction;

7. An increase in toluene fraction led to an increase in unburned hydrocarbon emissions;

8. An increase in toluene fraction had little effect on NOx emissions when the HCCI engine operated at a combustion phasing around or retarded relative to top dead center, but increased NO_x emissions if the engine operated at an advanced combustion phasing.

ACKNOWLEDGEMENTS

Funding for this work was provided by Natural Resources Canada through the Program of Energy Research and Development, PERD3B03.003 and National Research Council Canada through the internal Bioenergy Program.

REFERENCES

[1] Noguchi M, Tanaka Y, Tanaka T, Takeuchi Y. A study on gasoline engine combustion by observation of intermediate reactive products during combustion. 1979, SAE paper 790840. (https://saemobilus.sae.org/content/790840/)

[2] Onishi S, Jo SH, Shoda K, Jo PD, Kato S. Active thermo-atmosphere combustion (ATAC) - a new combustion process for internal combustion engines. 1979, SAE paper 790501. (https://saemobilus.sae.org/content/790501/)

[3] Najt PM, Foster DE. Compression ignited homogeneous charge combustion. 1983, SAE paper 830264. (https://saemobilus.sae.org/content/830264/)

[4] Westbrook CK. Chemical kinetics of hydrocarbon ignition in practical combustion systems. Proc Comb Inst 2000, 28, 1563-1577. (https://www.sciencedirect.com/science/article/pii/S0082078400805548/pdf?md5=d970b2f72d0acbaedbf21dea39482f53&pid=1-s2.0-S0082078400805548-main.pdf).

[5] Epping K, Aceves S, Bechtold R, Dec J. The potential of HCCI combustion for high efficiency and low emissions. 2002, SAE paper 2002-01-1923. (https://saemobilus.sae.org/content/2002-01-1923/)

[6] Hosseini V, Neill WS, Guo H, Dumitrescu CE, Chippior WL, Fairbridge C, Mitchell K. Effects of cetane number, aromatic content and 90% distillation temperature on HCCI combustion of diesel fuels. 2010, SAE paper 2010-01-2168. (https://saemobilus.sae.org/content/2010-01-2168/)

[7] Andrae J, Johansson D, Björnbom P, Risberg P, Kalghatgi G. Co-oxidation in the auto-ignition of primary reference fuels and n-heptane/toluene blends. Combustion and Flame 2005,140, 267-286. (https://www.sciencedirect.com/-science/article/pii/S0010218004002330/pdfft?md5=e72e94868d5b3c8f6323daa234aecf94&pid=1-s2.0-S0010218004002330-main.pdf) https://doi.org/10.1016/j.combustflame.2004.11.009

[8] Andrae JGG, Brinckb T, Kalghatgi GT. HCCI experiments with toluene reference fuels modeled by a semidetailed chemical kinetic model. Combustion and Flame 2008;155: 696-712. (http://ja6yb8mj3u.search.serialssolutions.com/?V=1.0&N=100&tab=JOURNALS&L=JA6YB8MJ3U&S=T_W_A&C=Combustion+and+Flame) https://doi.org/10.1016/j.combustflame.2008.05.010

[9] Sakai Y, Ozawa H, Ogura T, Miyoshi A, Koshi M, Pitz WJ. Effects of toluene addition to primary reference fuel at high temperature. 2007, SAE paper 2007-01-4104. (https://saemobilus.sae.org/content/2007-01-4104/)

[10] Xiao Z, Ladommatos N, Zhao H. The effect of aromatic hydrocarbons and oxygenates on diesel engine emissions. Proc Instn Mech Engrs 2000, 214D, 307-332. https://doi.org/10.1243/0954407001527448

[11] Szybist JP, Bunting BG. The effects of fuel composition and compression ratio on thermal efficiency in an HCCI engine. 2007, SAE paper 2007-01-4076. (https://saemobilus.sae.org/content/2007-01-4076/)

[12] Guo H, Hosseini V, Neill WS, Chippior WL, Dumitrescu CE. An experimental study on the effect of hydrogen enrichment on diesel fuelled HCCI combustion. Int J Hydrogen Energy

2011, 36, 13820-13830. (http://ja6yb8mj3u.search.serialssolutions.com/?V=1.0&N=100&tab=JOURNALS&L=JA6YB8MJ3U&S=T_W_A&C=International+Journal+of+Hydrogen+Energy) https://doi.org/10.1016/j.ijhydene.2011.07.143

[13] Guo H, Li H, Neill WS. A study on the performance of combustion in a HCCI engine using n-heptane by a multi-zone model. 2009, ASME Internal Combustion Engine Division 2009 Fall Technical paper ICEF2009-14117.

[14] Smith GP, Golden DM, Frenklach M, Moriarty NW, Eiteneer B, Goldenberg M. *et al*. http://www.me.berkeley.edu/-gri_mech/.

[15] Hsu BD. Heat release, cycle efficiency and maximum cylinder pressure in diesel engine: the use of an extended air cycle analysis. SAE Transactions 1984, 93, 4.766-4.778.

[16] Guo H, Liu F, Smallwood GJ. A numerical study on NO_X formation in laminar counterflow CH_4/air triple flames. Combustion and Flame 2005, 143, 282-98. (http://ja6yb8mj3u.search.serialssolutions.com/?V=1.0&N=100&tab=JOURNALS&L=JA6YB8MJ3U&S=T_W_A&C=Combustion+and+Flame) https://doi.org/10.1016/j.combustflame.2005.06.004

[17] Guo H, Neill WS, Li H. On the formation of NO_x and N_2O in an HCCI engine fuelled with n-heptane. 2010 Spring Technical Meeting of the Combustion Institute/Canadian Section, 2010.5, Ottawa, Canada.

Received on 9-7-2018 Accepted on 15-10-2018 Published on 7-12-2018

DOI: http://dx.doi.org/10.15377/2409-5826.2018.05.3